

Supplementary Materials

Crystalline bis(η^5 -cyclopentadienyl)bis(benzoato/carboxylato)titanium(IV) precursor-directed route to functional titanium dioxide nanomaterials

TUSHAR S. BASU BAUL, *^a RAJESH MANNE, ^a, EDWARD R. T. TIEKINK, **^b

^aCentre for Advanced Studies in Chemistry, North-Eastern Hill University, NEHU Permanent Campus, Umshing, Shillong 793 022, India

^bResearch Centre for Crystalline Materials, School of Science and Technology, Sunway University, 47500 Bandar Sunway, Selangor Darul Ehsan, Malaysia

Contents

Figure S1. (a) Digital camera micrograph of $[\text{Ti}(\eta^5\text{-C}_5\text{H}_5)_2(\text{O}_2\text{CC}_4\text{H}_3\text{-3-O})_2]$ (**3**) stored under an N_2 environment in a Schlenk tube, (b) stereomicroscopic images showing part of surface textures of bulk material of precursor **3**, (c) calcinated TiO_2 nanopowder and (d) TiO_2 nanopowder after ultrasonication.

Figure S2. (a) PXRD pattern of as-synthesized TiO_2 nanopowder annealed at 400 °C, 600 °C and 800 °C for anatase phase identification and (b) TEM micrographs of as-synthesized TiO_2 nanopowder annealed at 800 °C at 50 K magnification.

Figure S3. ^1H NMR spectrum of **1** in CDCl_3 .

Figure S4. ^{13}C NMR spectrum of **1** in CDCl_3 .

Figure S5. ^1H NMR spectrum of **2** in CDCl_3 .

Figure S6. ^{13}C NMR spectrum of **2** in CDCl_3 .

Figure S7. ^1H NMR spectrum of **3** in CDCl_3 .

Figure S8. ^{13}C NMR spectrum of **3** in CDCl_3 .

Figure S9. ^1H NMR spectrum of **4** in CDCl_3 .

Figure S10. ^{13}C NMR spectrum of **4** in CDCl_3 .

Figure S11. ^1H NMR spectrum of **5** in CDCl_3 .

Figure S12. ^{13}C NMR spectrum of **5** in CDCl_3 .

Figure S13. IR spectrum of **1** in KBr.

Figure S14. IR spectrum of **2** in KBr.

Figure S15. IR spectrum of **3** in KBr.

Figure S16. IR spectrum of **4** in KBr.

Figure S17. IR spectrum of **5** in KBr.

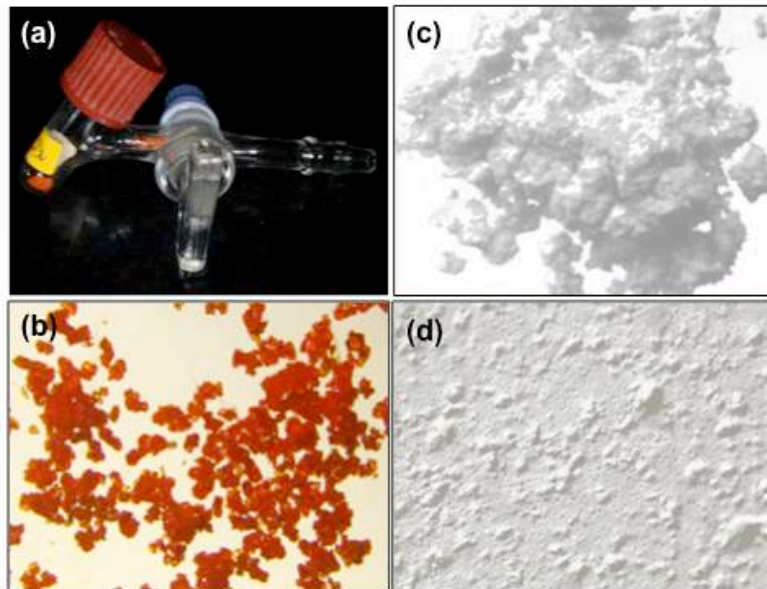


Figure S1. (a) Digital camera micrograph of $[\text{Ti}(\eta^5\text{-C}_5\text{H}_5)_2(\text{O}_2\text{CC}_4\text{H}_3\text{-3-O})_2]$ (**3**) stored under an N₂ environment in a Schlenk tube, (b) stereomicroscopic images showing part of surface textures of bulk material of precursor **3**, (c) calcinated TiO₂ nanopowder and (d) TiO₂ nanopowder after ultrasonication.

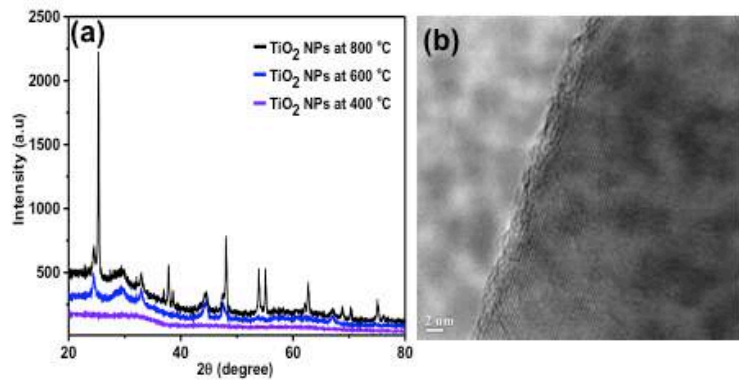


Figure S2. (a) PXRD pattern of as-synthesized TiO_2 nanopowder annealed at 400 °C, 600 °C and 800 °C for anatase phase identification and (b) TEM micrographs of as-synthesized TiO_2 nanopowder annealed at 800 °C at 50 K magnification.

COMP-1-1H.esp

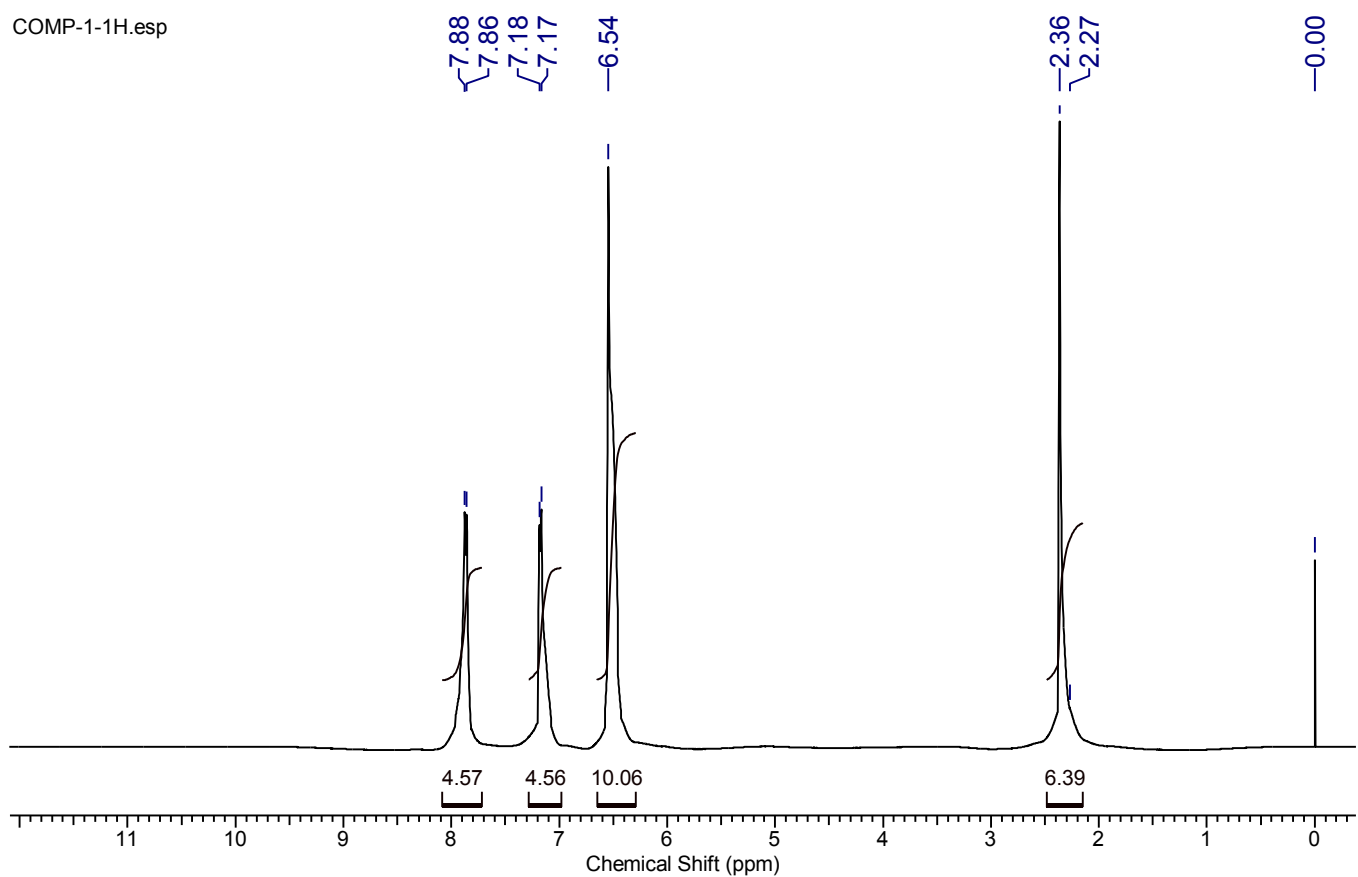


Figure S3. ¹H NMR spectrum of **1** in CDCl₃.

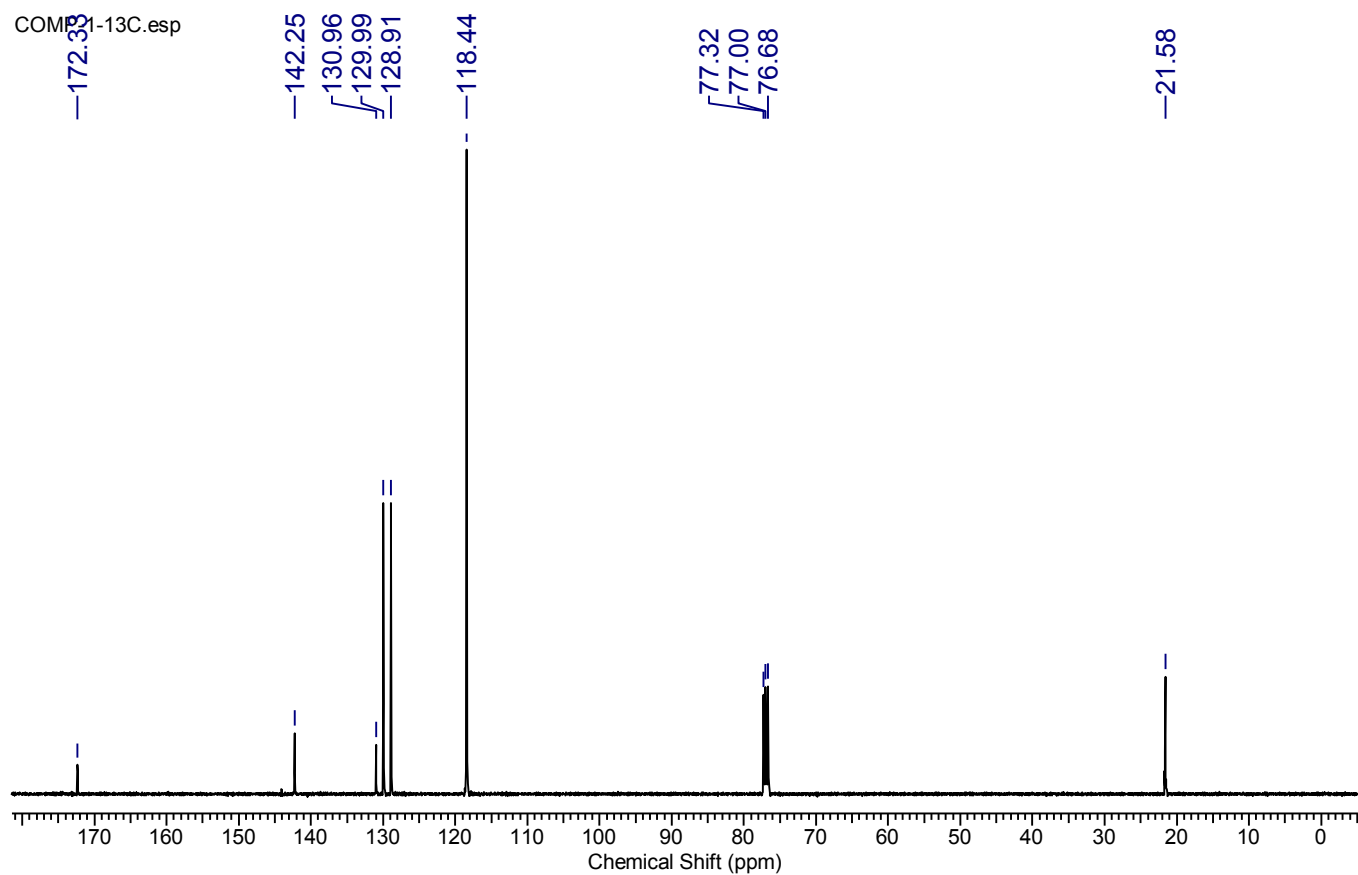


Figure S4. ^{13}C NMR spectrum of **1** in CDCl_3 .

COMP-2-1H.esp

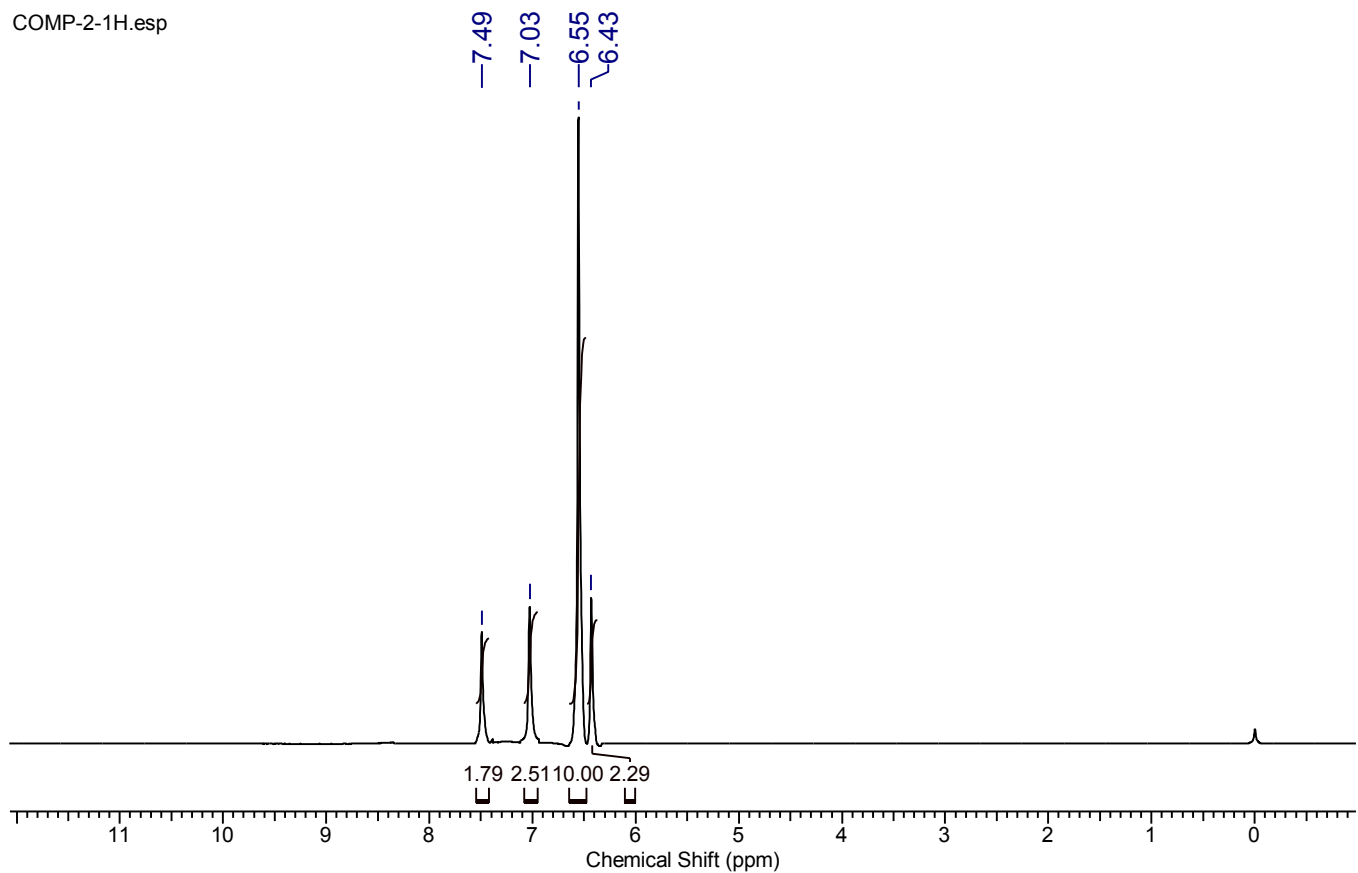


Figure S5. ¹H NMR spectrum of **2** in CDCl₃.

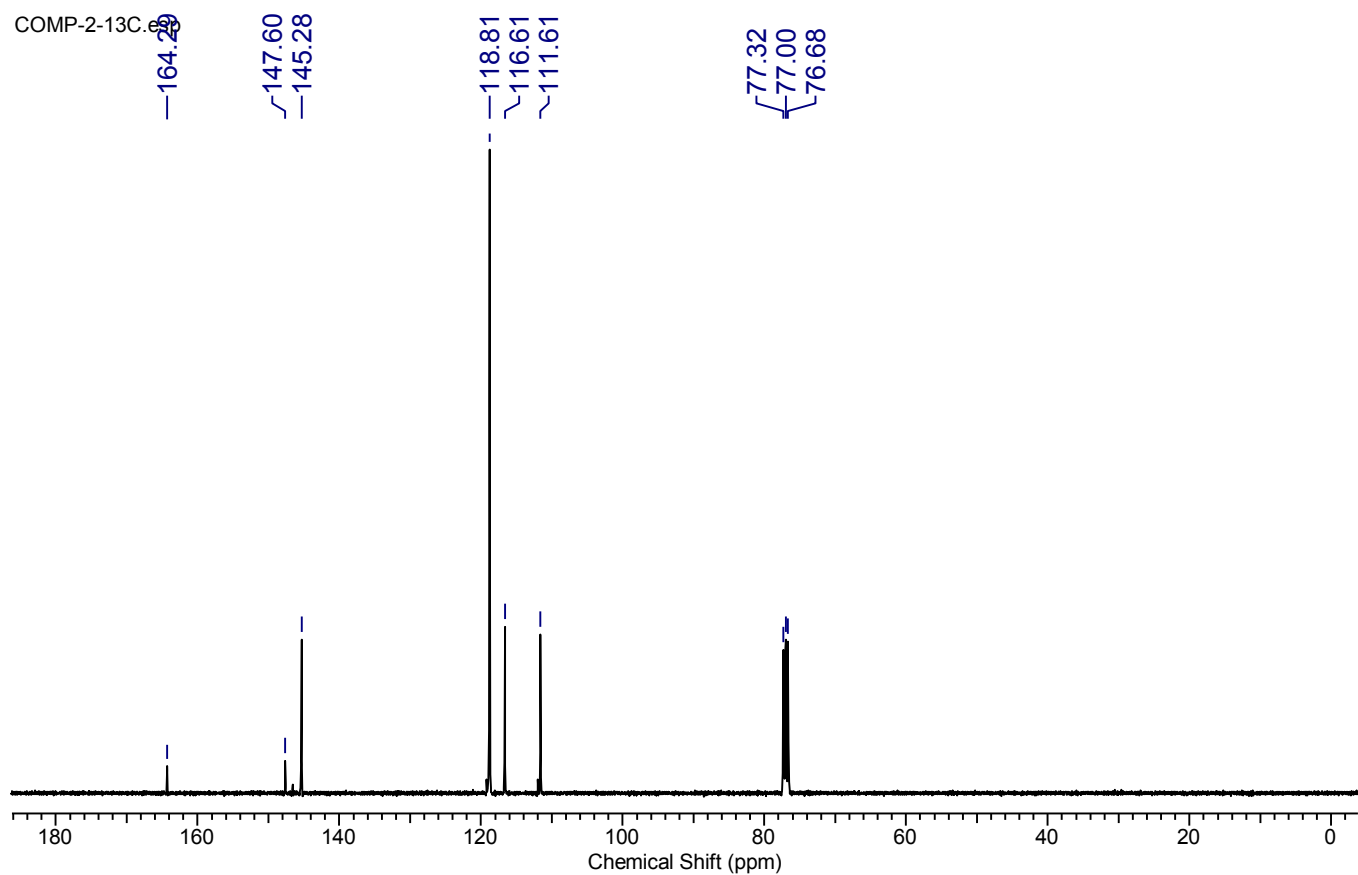


Figure S6. ^{13}C NMR spectrum of **2** in CDCl_3 .

COMP-3-1H.esp

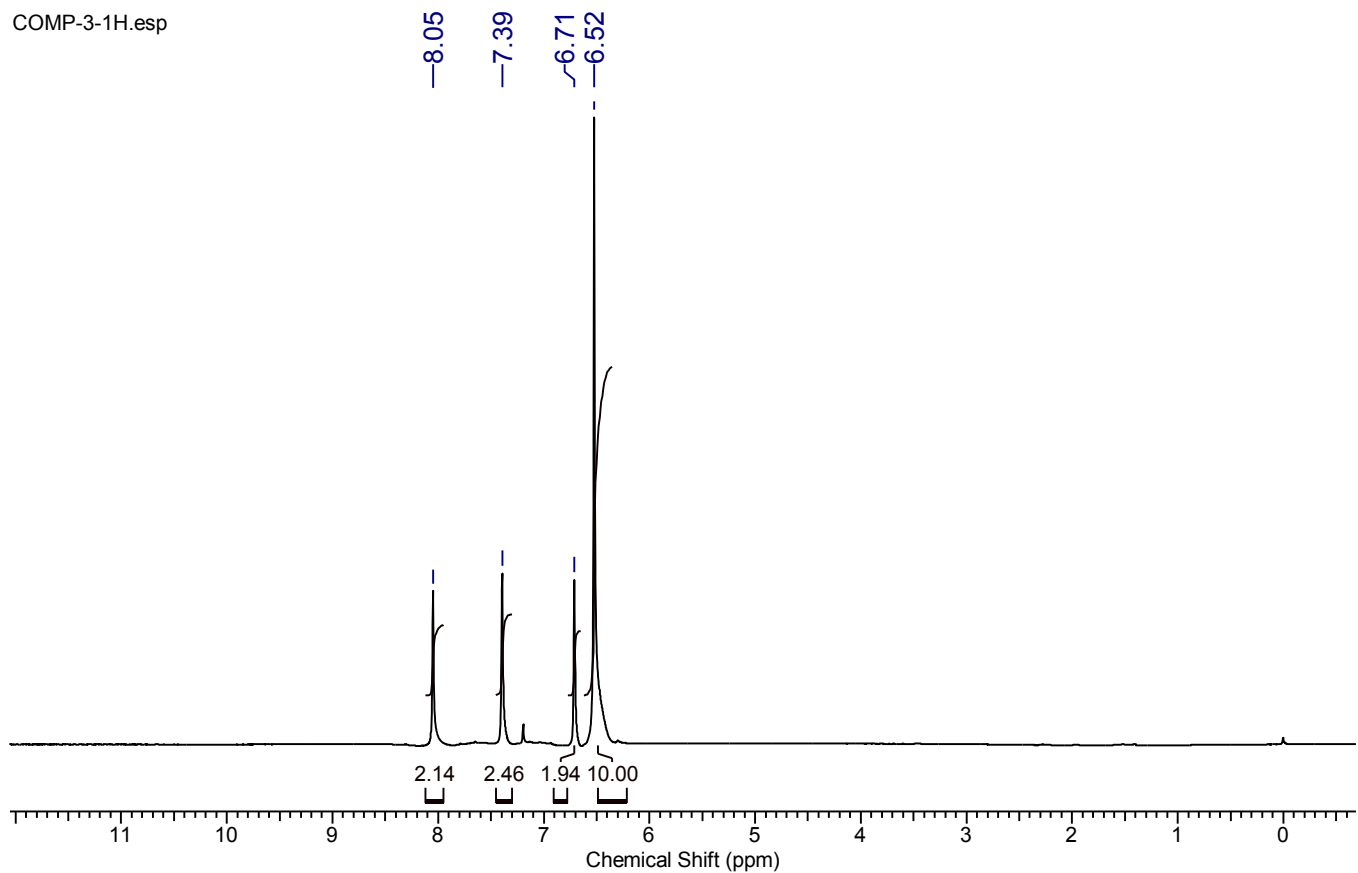


Figure S7. ¹H NMR spectrum of **3** in CDCl₃.

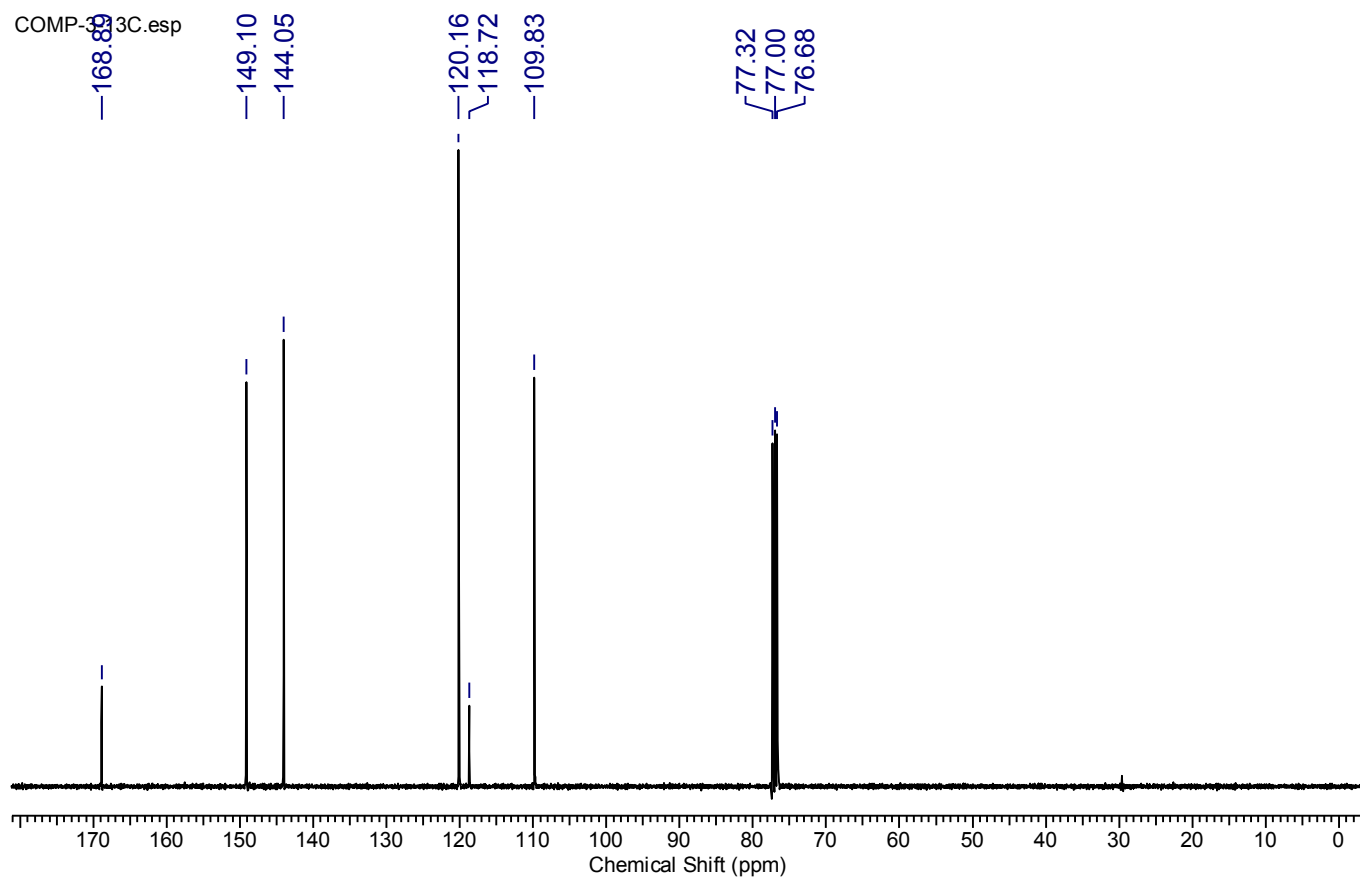


Figure S8. ^{13}C NMR spectrum of **3** in CDCl_3 .

COMP-4-1H.esp

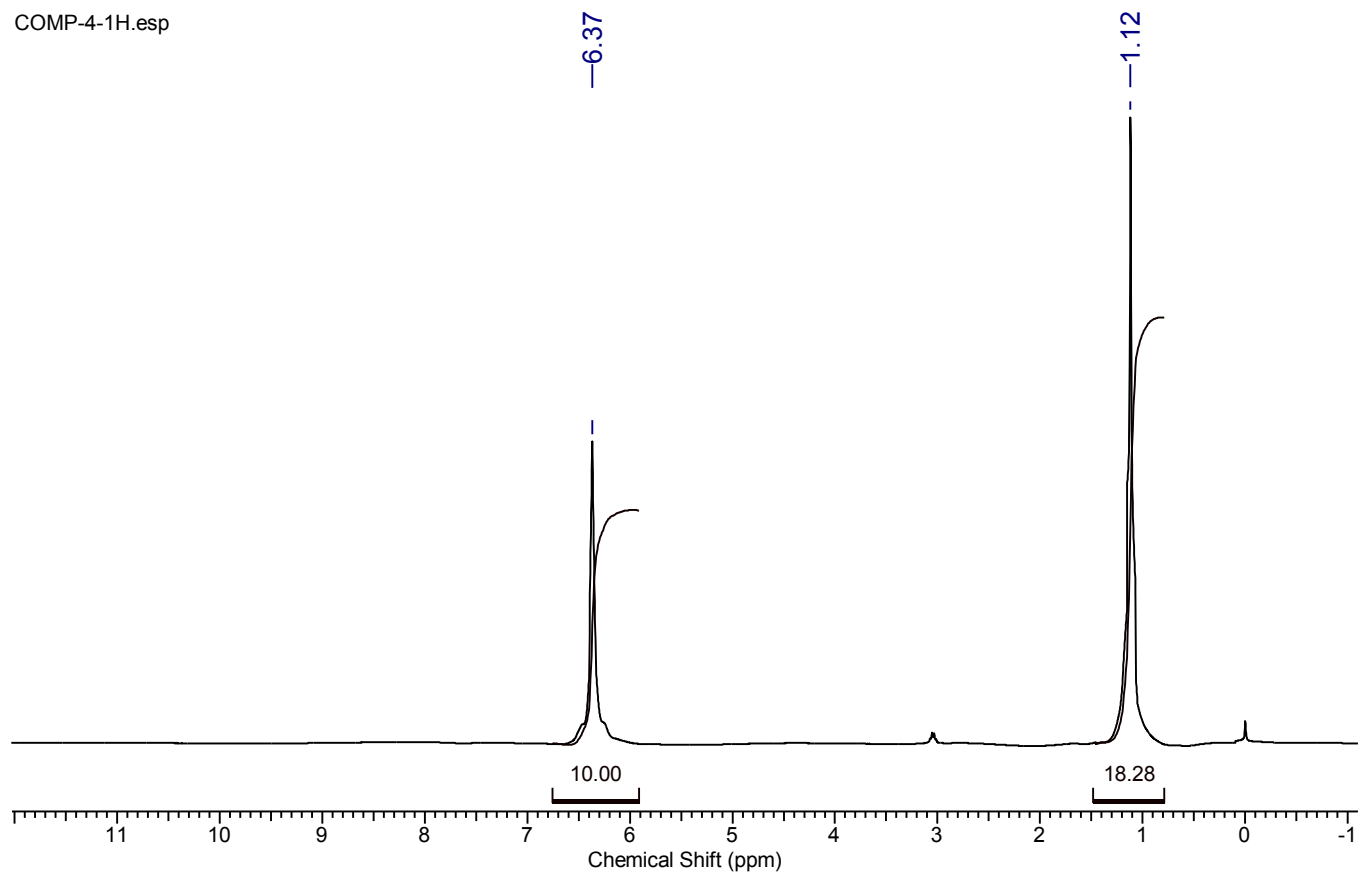


Figure S9. ¹H NMR spectrum of **4** in CDCl_3 .

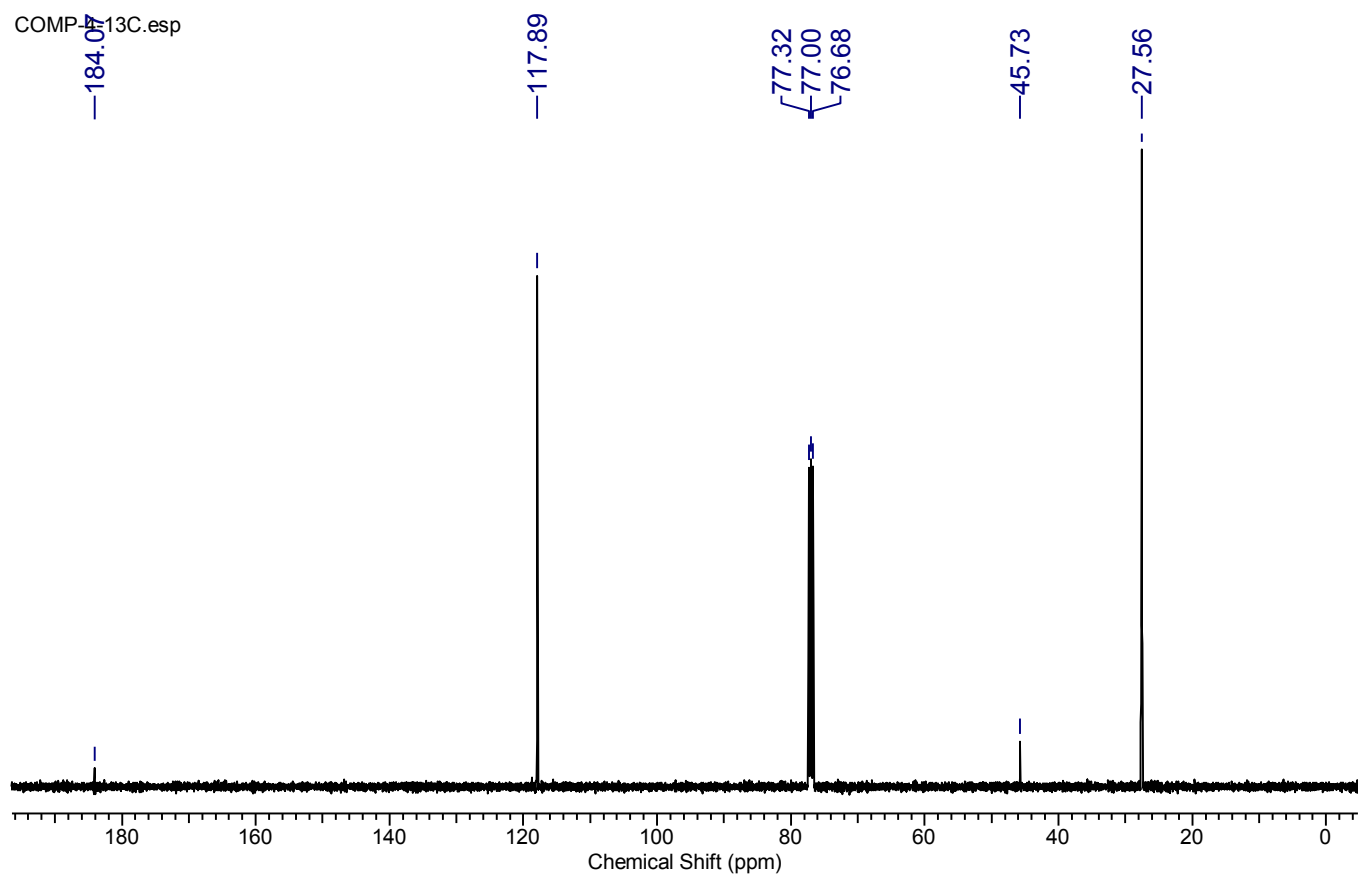


Figure S10. ¹³C NMR spectrum of **4** in CDCl₃.

COMP-5-1H.esp

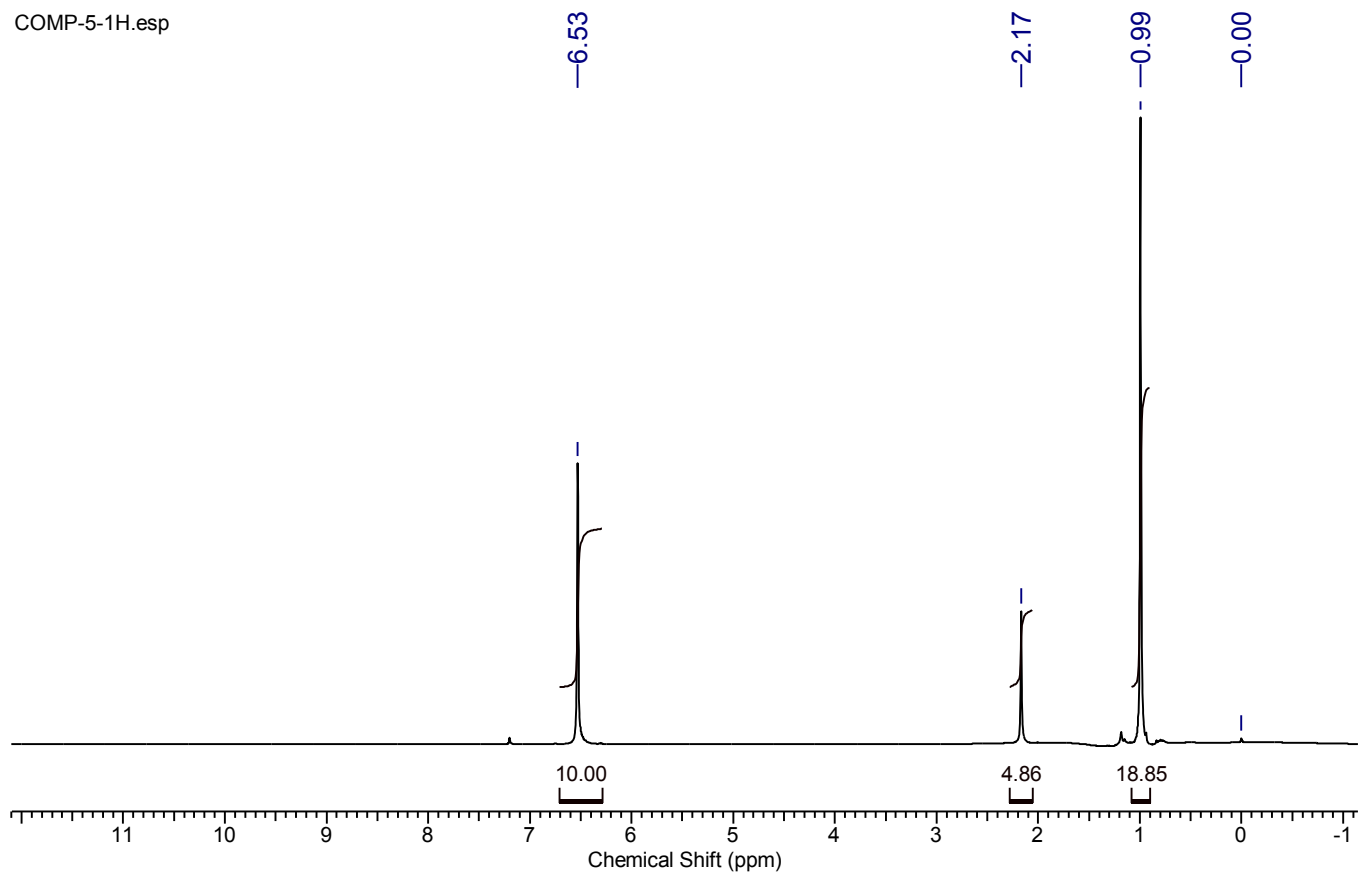


Figure S11. ¹H NMR spectrum of **5** in CDCl₃.

COMPLB-13C.esp

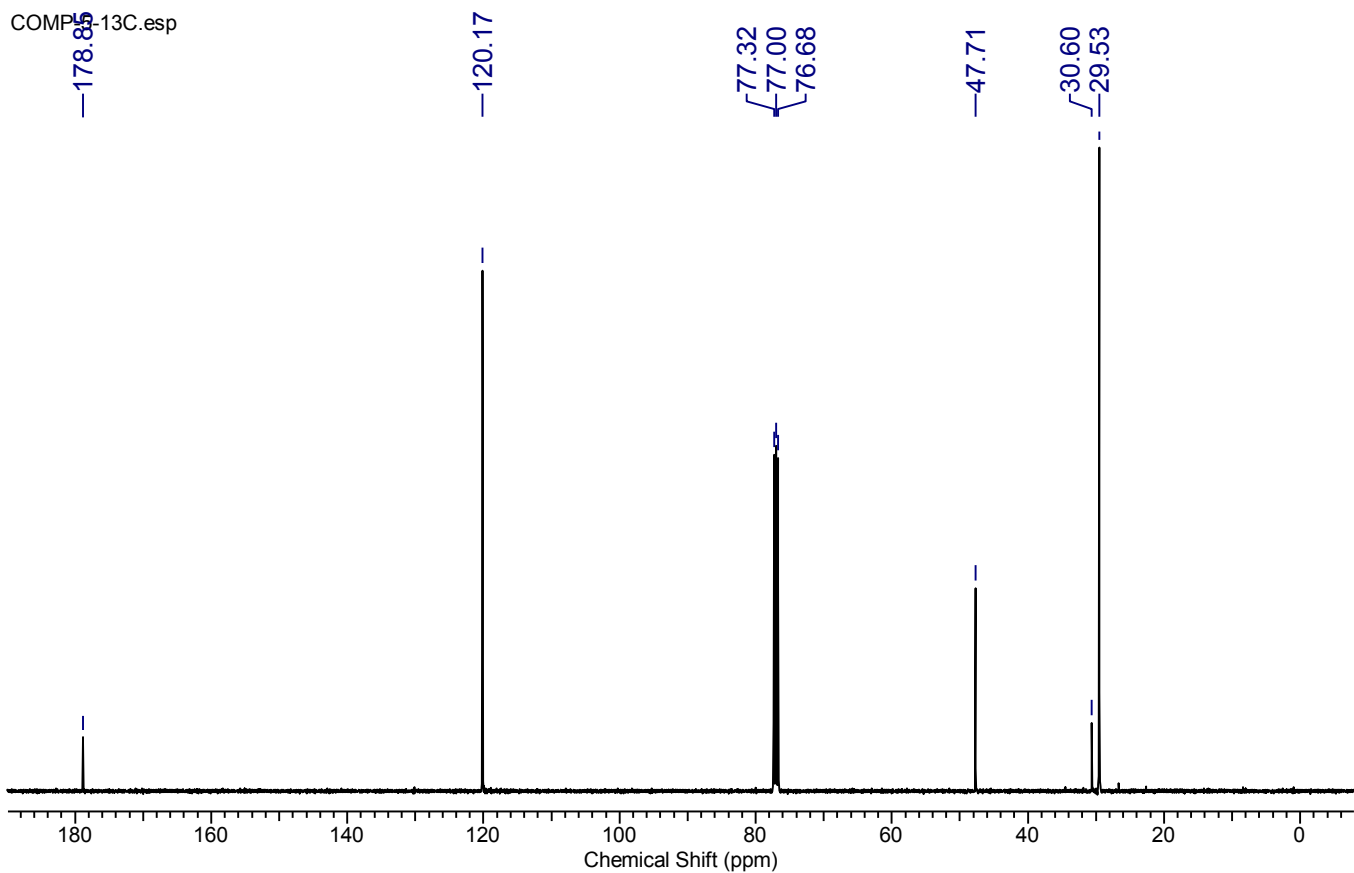


Figure S12. ¹³C NMR spectrum of **5** in CDCl_3 .

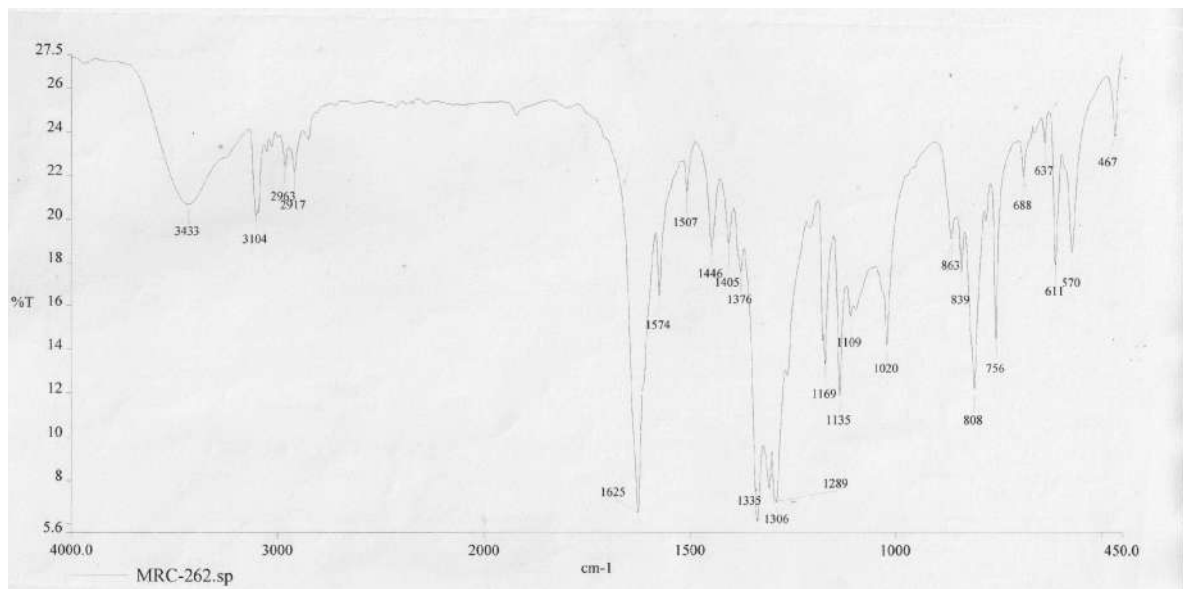


Figure S13. IR spectrum of **1** in KBr.

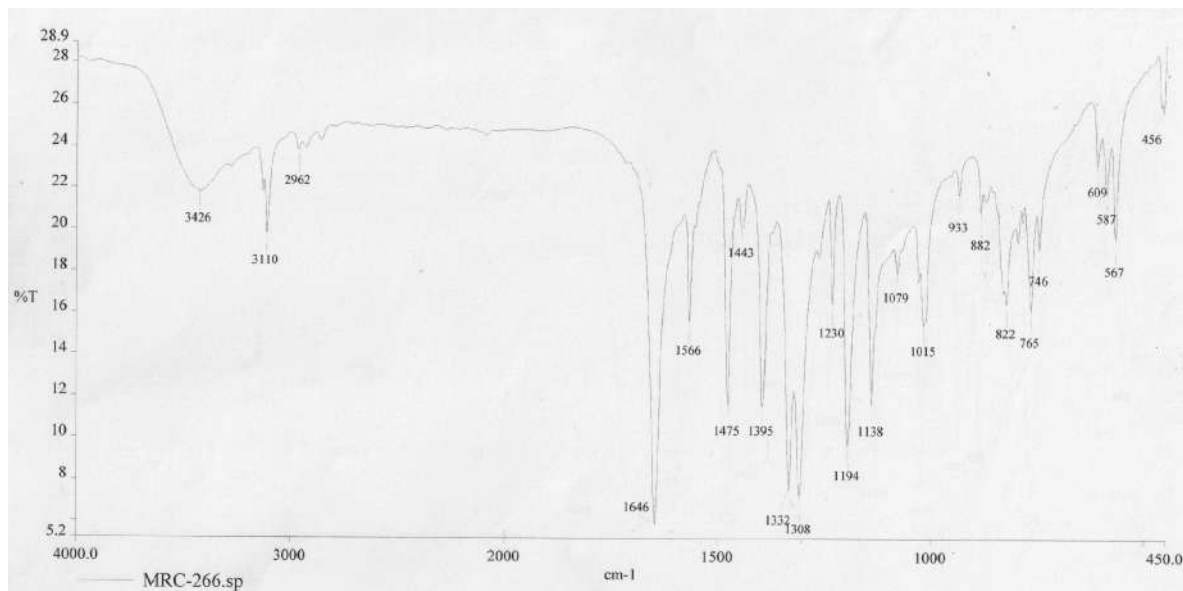


Figure S14. IR spectrum of **2** in KBr.

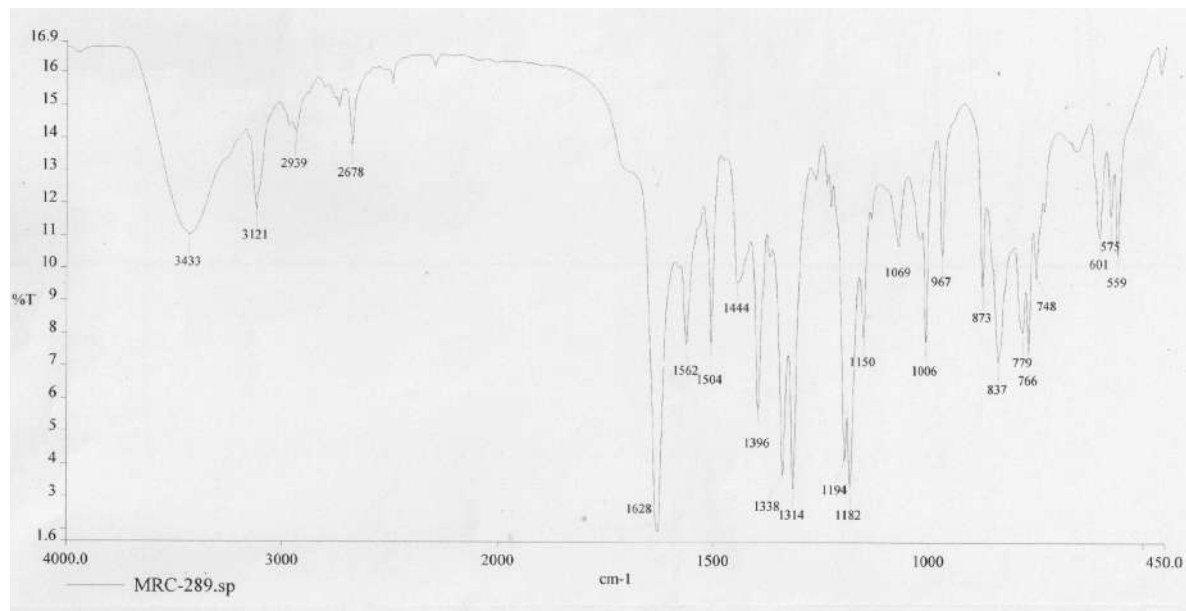


Figure S15. IR spectrum of **3** in KBr.

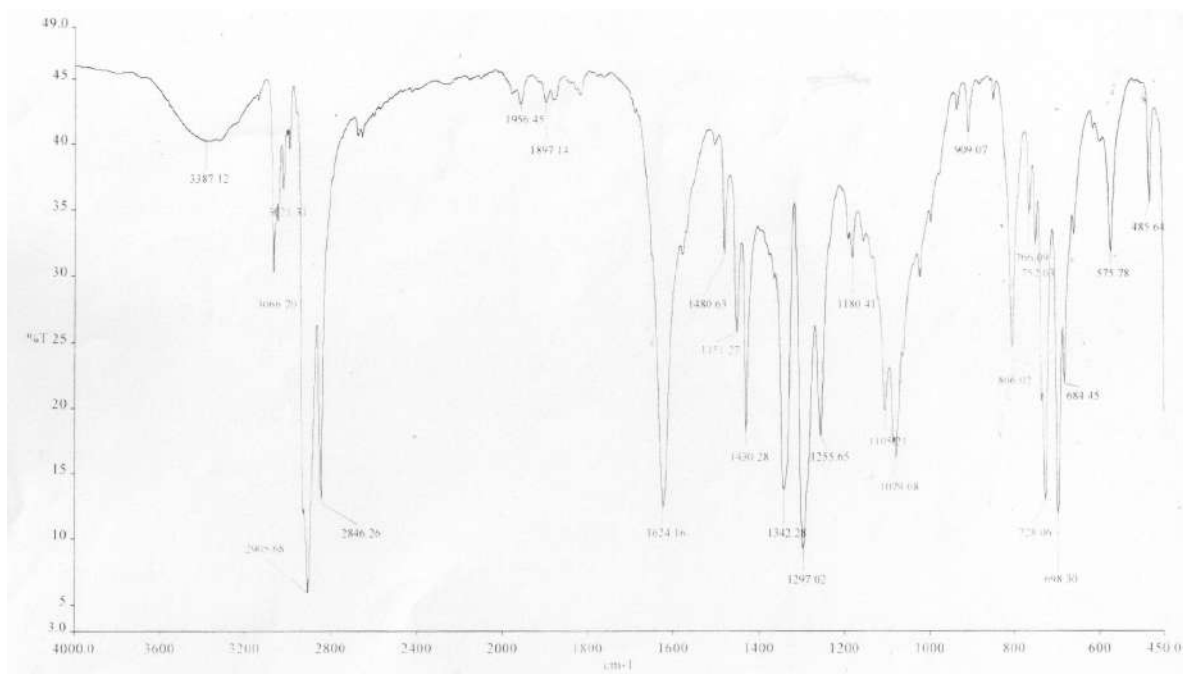


Figure S16. IR spectrum of **4** in KBr.

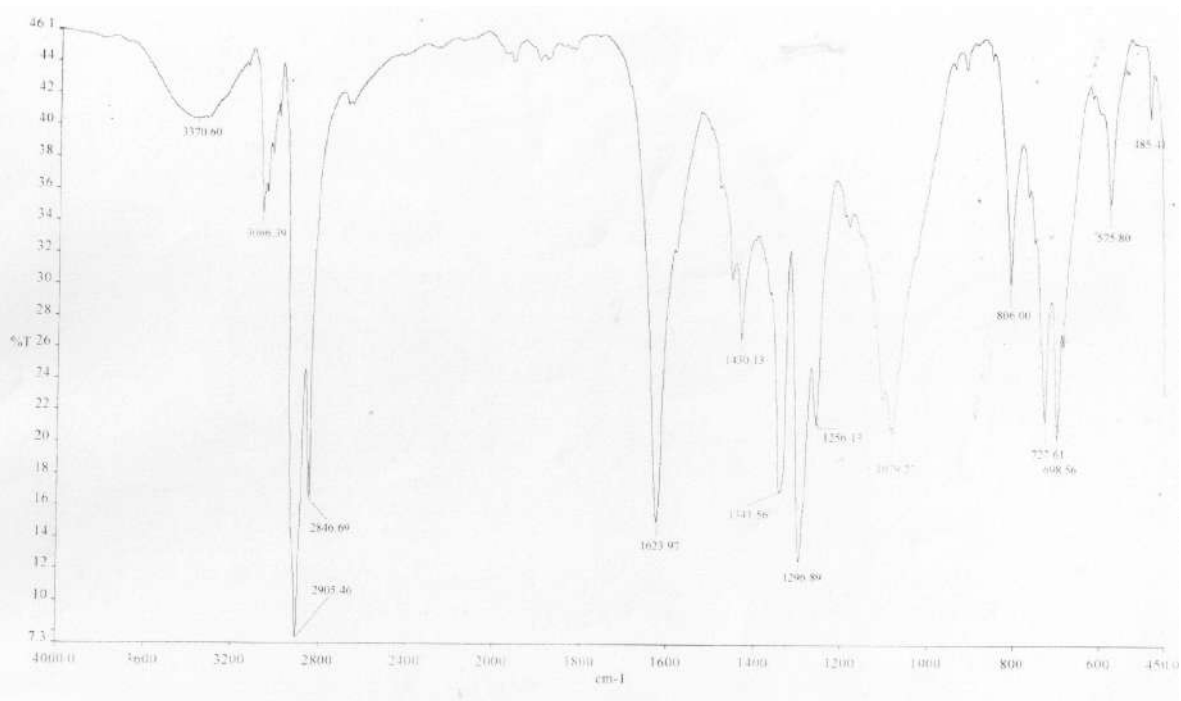


Figure S17. IR spectrum of **5** in KBr.